communications biology

A Nature Portfolio journal

Article

https://doi.org/10.1038/s42003-025-07806-5

Precise amplification-free detection of highly structured RNA with an enhanced SCas12a assay

Check for updates

Junqi Zhang[1,5], Wenhao Yin[1,2,5], Qingyuan Jiang[1,5], Wuxiang Mao[1] ✉, Wenwen Deng[1], Shuqi Jin[1], Xinping Wang[1], Ruyi He[3], Jie Qiao[3,4] ✉ & Yi Liu[1,2] ✉

The CRISPR/Cas12a system has revolutionized molecular diagnostics, yet the direct detection of RNA, particularly those with complex structures, remains a significant challenge. Here, we present an updated SCas12a system, termed SCas12aV2, which enables precise, amplification-free detection of highly structured RNA molecules. By optimizing the length of scaffold RNA, targeting asymmetric structures, and utilizing dsDNA-ssDNA hybrid activators, we have significantly reduced steric hindrance in the detection system, thereby markedly enhancing both sensitivity and kinetics compared to traditional DNA activators. The SCas12aV2 assay achieves a detection limit of 246 aM for pooled activators and 10 pM for single-site targeting, demonstrating high specificity for single nucleotide polymorphisms (SNPs). It successfully identifies viable bacteria and SARS-CoV-2 infections in clinical samples. The assay is versatile and can be applied to various Cas12a orthologs, including thermostable CtCas12a. This work advances molecular diagnostics by improving the accuracy and efficiency of RNA detection.

The emergence of CRISPR (Clustered Regularly Interspaced Short Palindromic Repeats)/Cas systems has dramatically transformed molecular biology, providing exceptional precision in genome editing and regulation[1,2]. Among the diverse Cas proteins, Cas12a[3,4] stands out as a type II-C RNA-guided DNA endonuclease. This enzyme can perform site-specific cleavage, known as *cis*-cleavage[5], on target double-stranded DNA (dsDNA). Additionally, it exhibits *trans*-cleavage activity on any single-stranded DNA (ssDNA) when a complementary sequence is identified within the spacer region of the crRNA. This unique capability has facilitated the development of highly sensitive and specific methods for nucleic acid detection, such as DETECTR[3,6] and HOLMES[4], highlighting their potential in enhancing point-of-care diagnostic tools.

To date, Cas12a-based detection tools have predominantly targeted DNA, with the notable exception of methods incorporating reverse transcription for RNA analysis[7–9]. Recently, several research groups have employed 'split-activator' strategies to engineer the Cas12a system for direct detection of RNA.[10–13]. For example, Jain et al. developed the SAHARA diagnostic method[10], enabling programmable RNA detection with Cas12a. This technique detects RNA at picomolar concentrations by utilizing a PAM-containing dsDNA as a seed region for the crRNA. Similarly, Moon et al. developed an asymmetric CRISPR assay[12] that leverages fragmented RNA/DNA targets for miRNA detection, obviating the need for pre-amplification. Our group has recently developed a diagnostic technique known as SCas12a assay[13], which combines Cas12a with a split crRNA comprising a 20-nt scaffold RNA and a variable 20-nt spacer RNA. This method harnesses the target RNA as the spacer, achieving sensitive, amplification-free, and multiplexed RNA biomarker detection. However, all these Cas12a-based RNA detection methods encounter challenges in accurately quantifying long RNA molecules with complex secondary structures. Therefore, it is imperative to develop more robust diagnostic tools in order to overcome these limitations.

In this study, we hypothesize that reducing steric hindrance between the highly structured RNA and the DNA activator will enhance the performance of the SCas12a assay. To test this hypothesis, we modified the split Cas12a system by repositioning the target RNA further from the protospacer adjacent motif (PAM) sequence. Our findings reveal that Cas12a can accommodate various lengths of split scaffold RNAs, with a 26-nucleotide scaffold RNA (S6) being optimal for RNA detection. Additionally, we found

[1]State Key Laboratory of Biocatalysis and Enzyme Engineering, School of Life Sciences, Hubei University, Wuhan, Hubei, 430042, China. [2]BravoVax Co., Ltd, Wuhan, Hubei, 430075, China. [3]Pilot Base of Food Microbial Resources Utilization of Hubei Province, School of Life Science and Technology, Wuhan Polytechnic University, Wuhan, Hubei, 430023, China. [4]State Key Laboratory of Esophageal Cancer Prevention & Treatment, Department of Oral and Maxillofacial Surgery, The First Affiliated Hospital of Zhengzhou University, Zhengzhou University, Zhengzhou, 450001, China. [5]These authors contributed equally: Junqi Zhang, Wenhao Yin, Qingyuan Jiang. ✉e-mail: wxmao@hubu.edu.cn; jieqiao@whpu.edu.cn; yiliu0825@hubu.edu.cn

that targeting asymmetric RNA structures and utilizing a PAM-containing dsDNA-ssDNA hybrid activator significantly improves detection efficiency and sensitivity. We designate this improved assay as SCas12aV2, which achieves a limit of detection (LoD) of 10 pM for single-site targeting and 246 aM for multi-site targeting. Furthermore, SCas12aV2 enables the effective detection of complex structures within the SARS-CoV-2 RNA target, which are inaccessible to SHERLOCK using Cas13a[14,15]. We also demonstrate the successful application of SCas12aV2 for identifying viable bacterial populations[16] and detecting SARS-CoV-2 infections in patients[17]. Collectively, we have developed a highly efficient, amplification-free Cas12a-based method for the rapid, cost-effective, and accurate detection of RNA substrates with diverse sequences and complex structures.

Results

Cas12a tolerates different lengths of split scaffold RNA for *trans*-cleavage activity

AsCas12a is an ortholog of Cas12a that originates from *Acidaminococcus sp. BVL36*. The mature crRNA for AsCas12a is 40 nucleotides in length, consisting of a 20-nt scaffold and a complementary 20-nt spacer. Leveraging a split crRNA as illustrated in Fig. 1a, we have recently established the SCas12a assay for the direct detection of RNA molecules[13]. Nonetheless, this method still faces limitations in analyzing long RNA molecules with intricate secondary structures. We hypothesized that alleviating the steric hindrance between the highly structured RNA and the DNA activator could potentially create sufficient space for accessibility of the RNA substrate, thereby overcoming these limitations. In this study, we initially optimized the design of the split Cas12a system by relocating the target RNA downstream of the PAM sequence (Fig. 1b), which would provide additional integration space. This modified system was designated as SCas12aV2.

To activate the *trans*-cleavage activity of Cas12a, we initially assessed the viability of employing scaffold and spacer RNAs with varied nucleotide sequences. We then determined the optimal scaffold length for Cas12a by synthesizing a series of scaffold RNAs (S3 to S12), each varying in length from 23 to 32 nucleotides (Fig. 1c). For instance, using the S6 scaffold, we utilized a 14-nt spacer in conjunction with complementary target activators, which were presented as either dsDNA or ssDNA, to evaluate the enzyme's *trans*-cleavage activity on non-specific ssDNA targets. The electrophoresis data included either a 59-bp dsDNA target (Fig. 2a) or a 59-nt ssDNA target (Fig. 2b), along with a 42-nt ssDNA reporter. Collectively, these findings demonstrate the restoration of the full *trans*-cleavage capability of the wild-type Cas12a RNP. Subsequently, the real-time fluorescence kinetic data (Fig. 2c, d) are in accordance with these PAGE results, indicating that the ssDNA activator is more effective at inducing the *trans*-cleavage activity of Cas12a. Additionally, our analysis revealed no sequence dependence for scaffold RNAs with different G-C % (Supplementary Fig. S1). Based on these results, we have chosen the S6 scaffold with a consistent sequence (Table S1), for all subsequent experiments unless specified otherwise.

Next, we conducted in vitro *trans*-cleavage fluorescence assays by systematically combining a scaffold RNA with an ssDNA activator (Fig. 1c). We utilized a segment of the hepatitis C virus (HCV) polypeptide precursor RNA (Fig. 3a), characterized by its complex secondary structures, as the substrate. Specifically, we targeted four distinct regions within the HCV fragment for detection. Our findings indicate that scaffold RNAs S3 to S8 were capable of recognizing the highly structured RNA substrates (Fig. 3b, c), whereas scaffold RNAs S9 to S12 were not. Among the four target sites, S6 scaffold RNA displayed the highest detection sensitivity. Consequently, the S6 scaffold RNA was chosen for the SCas12aV2 assay. For reference, the 20-nt scaffold RNA previously employed in the SCas12a assay is denoted as S0.

Enhanced sensitivity of RNA detection through recognition of asymmetric structures

The newly developed SAHARA[10] and SCas12a assay[13] enable the direct detection of RNA, yet they are limited in their ability to identify RNA substrates with intricate secondary structures, such as stems and cloverleafs. Although these methods are adept at detecting the 5'-head nucleotides, such as the F1 region in the HCV fragment, they struggle with the F2 to F4 regions which are defined by their stem structures (Fig. 3a). We hypothesized that the SCas12aV2 system could improve the accessibility of the Cas12a-scaffold RNA complex, thereby facilitating additional spatial accommodation for RNA binding. To test this, we first performed experiments targeting the symmetrical stem structures (Fig. 4a). The results demonstrated significant reductions in detection efficiency for these regions compared to F1 (Fig. 4b), likely attributable to the diminished binding affinity of the symmetrical structure towards its complementary S6 ssDNA activator. To address this issue, we then designed a series of S6 ssDNA activators specific to the asymmetric structures (Fig. 4a). The modifications resulted in significant enhancements in the fluorescence intensity (Fig. 4b), which are comparable to the levels observed for F1. Consequently, the integration of SCas12aV2 assay with asymmetric RNA targets facilitates the highly sensitive detection of intricate secondary structures within long RNA molecules.

Next, leveraging the AlphaFold Server, we employed predictive structural modeling to analyze the complex comprising Cas12a, either the S0 or S6 scaffold, the ssDNA activator, and the F2 of HCV segment. The results elucidate the underlying structural basis for the heightened sensitivity observed in the SCas12aV2 assay. As illustrated in Fig. 4c, the binding of Cas12a/S6 scaffold complex to both ssDNA and RNA targets induces an activated state, thereby facilitating a highly adaptable conformation of the RNA target. The active center of Cas12a in this case exhibits flexibility, which enables efficient access of ssDNA probes to the RuvC domain for *trans*-cleavage. In contrast, the HCV target within the Cas12a/S0 scaffold complex adopts a considerably more rigid conformation, impeding effective accessibility of ssDNA probes to the RuvC domain. Recently, Huang et al.[18] demonstrate that upon binding of split DNA activators adjacent to the PAM to the Cas12a RNP, a ternary complex form that can capture and interact with distal split DNA activators to achieve synergistic effects. The conclusion aligns with our experiment and predictive results, perfectly explaining the inability to detect the F2 region of the HCV target using the S0 scaffold, while detection remains feasible with the S6 scaffold.

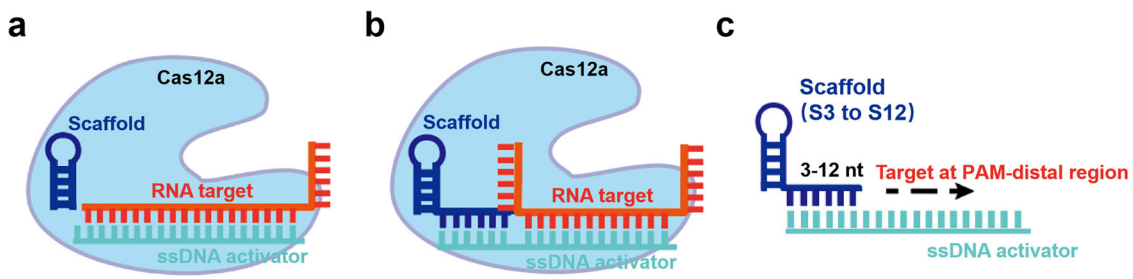


Fig. 1 | Combined use of split scaffold RNA and ssDNA activators enabling RNA detection by Cas12a. a Schematic illustration of the SCas12a assay by using a 20-nt scaffold RNA and ssDNA activator for RNA detection. **b** Schematic representation of Cas12a activated by combinations of scaffold RNA, ssDNA activator, and RNA target. **c** Extension of the scaffold RNA, ranging from 23 to 32 nt (S3 to S12), to detect RNA at PAM-distal region.

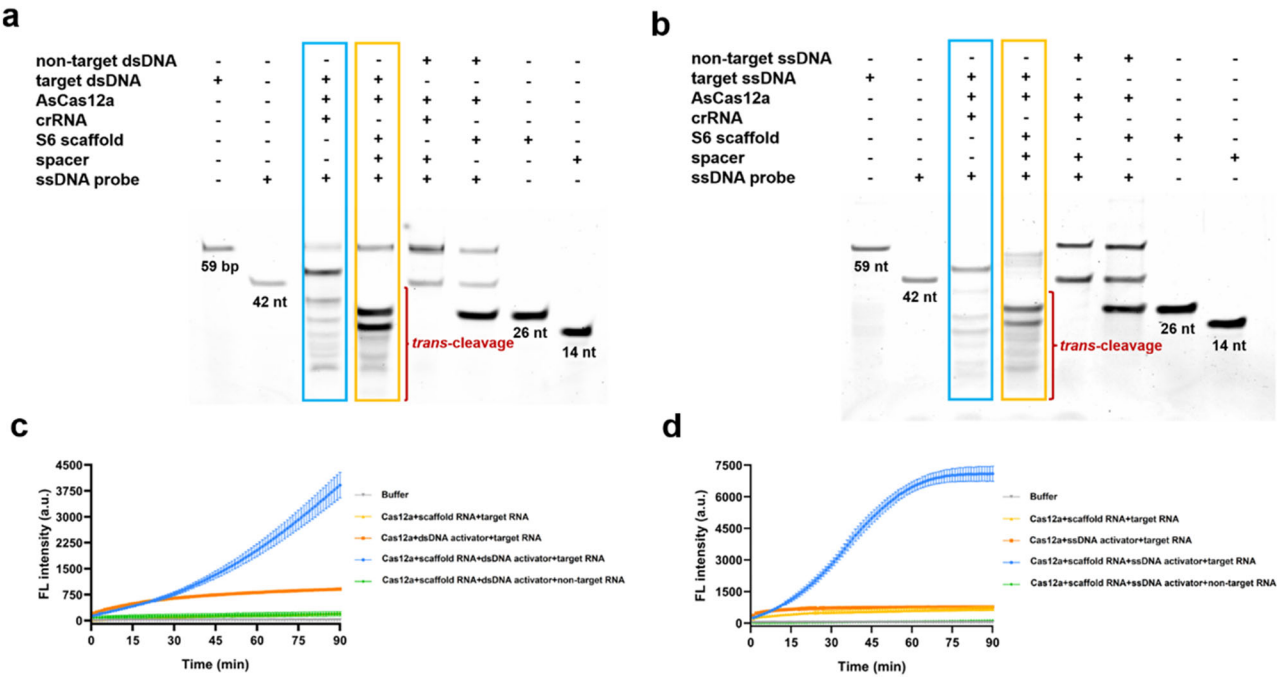


Fig. 2 | Comparison of the *trans*-cleavage activity between Cas12a with WT crRNA and split crRNA (26-nt scaffold + 14-nt spacer). **a** *Trans*-cleavage of ssDNA probes by Cas12a complexed with WT crRNA (blue) and split crRNA (orange) in the presence of target or non-target dsDNA. The reactions contained 50 nM Cas12a, 100 nM of either crRNA or split RNA,10 nM of either complementary dsDNA activators or non-target dsDNA substrates, as well as 20 nM ssDNA probes. **b** *Trans*-cleavage of ssDNA probes by complexed with WT crRNA (blue) and split crRNA (orange) in the presence of target or non-target ssDNA. The reactions contained 50 nM Cas12a, 100 nM of either crRNA or split RNA, 10 nM of either complementary ssDNA activators or non-target ssDNA substrates, as well as 20 nM ssDNA probes. **c**, **d** Detection of target RNA by Cas12a complexed with scaffold RNA and dsDNA (**c**) or ssDNA (**d**) activators. The reaction mixtures were incubated for 60 min at 37 °C and contained 250 nM of Cas12a, 500 nM of scaffold RNA, 10 nM target or non-target RNA substrates, 500 nM of dsDNA or ssDNA activators (dsDNA for **c** and ssDNA for **d**), and 1000 nM of fluorescent probes. For all panels, experiments were conducted in triplicate, and error bars represent the mean ± SD (n = 3). Supplementary Data 1 are provided as a Supplementary Data 1 file.

Enhanced capability of the SCas12aV2 assay by utilizing a dsDNA-ssDNA hybrid activator

To date, almost all detection methods based on Cas12a employ dsDNA or ssDNA as activators (Fig. 5a). We hypothesized that employing a dsDNA-ssDNA hybrid activator (Fig. 5a), capable of interacting with both the scaffold and target RNAs, might enhance the efficiency of Cas12a's collateral cleavage activity. To distinguish this approach from the ssDNA-based method that uses S6 activator, we termed this hybrid activator as S6.1. Initially, we conducted in vitro collateral cleavage assays employing a scaffold RNA, a hybrid activator, and a 150-nt RNA segment originating from the human TP53 gene (Fig. 5b-h). The data revealed that the S6.1 activators displayed significantly higher fluorescence intensity compared to the S6 activators at all five targeting sites (Fig. 5g). Notably, the F4 and F5 sites, which were previously undetectable with ssDNA activators, became detectable with these hybrid activators. Furthermore, the hard-to-detect symmetrical structures at F3 and F6 were also effectively recognized, indicating that the hybrid DNA activator is compatible with a wider range of RNA substrate spatial configurations. In contrast, the SCas12a assay utilizing the S0 activator failed to detect these targets.

Next, we evaluated the kinetic properties of fluorescence assays utilizing S0, S6, or S6.1 activators. The results indicate that the catalytic reactions mediated by S6.1 are much faster than those mediated by S6 activators (Fig. 5b–g). The potential to improve the speed of point-of-care testing (POCT) for RNA molecules, especially those with long lengths and complex secondary structures, is highlighted by this observation. To confirm the method's universality, we used the SCas12aV2 assay with S6.1 activators to detect various RNA substrates. The transcript from the human papillomavirus (HPV), known for its complex secondary structures (Fig. 5j), was tested and showed detectability of all targets except F4 (Fig. 5k). Finally, we demonstrate that SCas12aV2 facilitates the efficient detection of complex regions within the SARS-CoV-2 target (Supplementary Fig. S2), which are inaccessible to Cas13a-based SHERLOCK method[17].

In conclusion, the dsDNA-ssDNA hybrid activator significantly enhances the performance of the fluorescence assay compared to traditional dsDNA and ssDNA activators. This improvement is attributed to the hybrid's ability to promote stronger and more stable interactions between the RNA substrate and the active site of Cas12a. A key aspect of this mechanism is the optimal conformation achieved after substrate matching. Cas12a recognizes the PAM-containing double-stranded region, unwinds the DNA to form an R-loop structure, thereby positioning the target strand in proximity to S6 while excluding the non-target strand from the enzyme's active site. The formation and stabilization of the R-loop are crucial for cleavage activation, a process that is more intricate than single-strand cleavage and relies heavily on Cas12a's conformational changes and interactions with its protein domains. Moreover, Cas12a's cleavage efficiency is closely linked to the primary cleavage sites located at positions 18-19 on the non-target strand and 23-24 on the target strand. The hybrid activator is specifically designed to avoid these sites, thereby fully activating collateral cleavage activity and enhancing turnover efficiency. Consequently, unless otherwise specified, this hybrid activator is utilized in subsequent sections. These results further highlight the potential of the SCas12aV2 assay as a robust tool for RNA detection.

Application of the SCas12aV2 assay to different Cas12a orthologs

The orthologs of Cas12a, LbCas12a[19] and CtCas12a[20], derived from *Lachnospiraceae bacterium ND2006* and *Clostridium thermobutyricum* respectively, are referred to as Lb and Ct in this context. To date, AsCas12a and LbCas12a have seen widespread application in nucleic acid detection. Of particular interest is the recently discovered thermostable CtCas12a, which

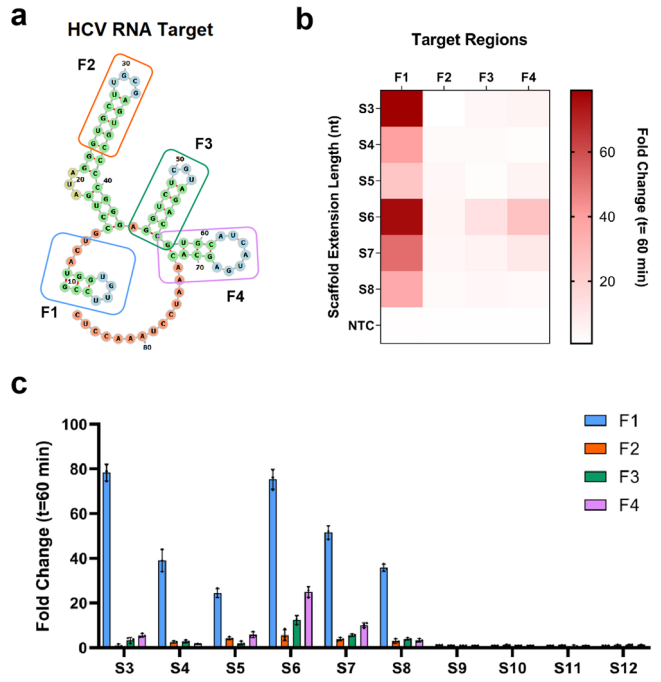


Fig. 3 | Detection of distinct regions within an HCV fragment by Cas12a complexed with S6 scaffold and ssDNA activator. a Schematic of an HCV RNA fragment with four target regions. The predicted secondary structure was determined by NUPACK software. **b** Heat map representing fold change with respect to NTC at $t = 60$ min of an in vitro *trans*-cleavage fluorescence assay using the scaffold S3 to S8. **c** Comparison of the different scaffold RNAs (S3 to S12) and ssDNA activators for HCV target. The plot represents the fold change in fluorescence intensity normalized to the NTC at $t = 60$ min ($n = 3$). Supplementary Data 1 are provided as a Supplementary Data 1 file.

exhibits activity over a broad temperature range[20], extending from 17 to 77 °C. Our investigation focused on assessing the performance of these Cas12a orthologs in the SCas12aV2 assay. The results demonstrate that the hybrid dsDNA-ssDNA activator is optimal for engaging all Cas12a orthologs with TP53 RNA targets (Fig. 6). Specifically, LbCas12a exhibits a significantly lower detection efficiency compared to AsCas12a and CtCas12a, being approximately 10-fold and 20-fold less sensitive, respectively. This reduced sensitivity suggests that LbCas12a's active site has a higher specificity for RNA substrate structure. Additionally, CtCas12a demonstrates enhanced sensitivity in detecting RNA with complex structures and high GC content, especially at its optimal temperature of 55 °C. The increased activity of CtCas12a is likely attributed to the greater conformational flexibility of RNA at elevated temperatures. These findings suggest that the selection of Cas12a orthologs can be optimized for specific requirements within the SCas12aV2 assay, thereby enhancing detection capabilities.

The limit of detection for RNA detection by SCas12aV2 assay

We first employed the fluorescence-based SCas12aV2 assay for RNA detection without the need for amplification. The sensitivity was evaluated by employing a panel of dsDNA-ssDNA hybrid activators targeting specific RNA segments derived from human immunodeficiency virus (HIV) (Fig. 7a) and TP53 (Supplementary Fig. S3). Regarding the HIV RNA target, we generated a gradient of RNA target concentrations ranging from 246 aM to 10 nM. The limit of detection (LoD) for each target was determined by introducing an excess amount of these activators, resulting in an established LoD of 100 fM as described in detail in the Methods section. For the TP53 RNA targets, distinct regions exhibited varying LoDs ranging from 3.6 pM to 86 pM (Supplementary Fig. S3). Overall, the average LoD of 10 pM demonstrates the assay's efficacy in detecting RNA with diverse secondary structures. It has been reported that Cas12a, when utilizing full-length crRNA, can detect RNA substrates[21]; however, the limit of detection (LoD) for this assay is relatively high at ~3 nM. Furthermore, our findings indicate that conventional Cas12a fails to detect the F1 to F3 regions of P53 RNA (Fig. S4). These results suggest that Cas12a exhibits limitations in detecting highly structured regions within long RNA molecules.

In the end, we have successfully established a linear correlation between the fluorescence intensity and the concentration of TP53 RNA standards (Supplementary Fig. S5). This validation confirms the robustness of our methodology for quantifying RNA. Moreover, employing a combination of activators that target multiple regions of the identified RNA enables a significant enhancement in LoD by 100- to 1000-fold. For instance, we employed a panel of activators targeting four distinct regions within the RNA of SARS-CoV-2 virus (Supplementary Fig. S6), resulting in an estimated LoD value of 246 aM. Finally, we demonstrate that SCas12aV2 facilitates the efficient detection of complex regions within the SARS-CoV-2 target, which are inaccessible to Cas13a-based SHERLOCK method[17].

In addition to fluorescence readout, we also assessed the sensitivity of SCas12aV2 using a rapid lateral flow assay (LFA) readout, achieving an impressive limit of detection (LoD) as low as 1 pM (Fig. 7b). Collectively, these experiments validate the efficient and unbiased capability of the SCas12aV2 assay in detecting RNA targets.

SCas12aV2 assay exhibits exceptional mutation detection specificity

In our recent research, we established that the SCas12a assay possesses remarkable sensitivity for the detection of single nucleotide polymorphisms (SNPs) within miRNAs[13]. Based on these findings, the current study aimed to evaluate the sensitivity of the SCas12aV2 assay for SNP detection in long RNA molecules. Utilizing an HIV-derived fragment as a case study, we engineered 14-nt ssDNA activators (S6) and dsDNA-ssDNA DNA hybrid activators (S6.1) with single-point mutations for SCas12aV2 detection. For comparative analysis, we also designed 20-nt ssDNA activators with corresponding mutations for use with the DETECTR, employing complete crRNA (Fig. 8). The specificity of target recognition was ascertained by quantifying the relative fluorescence enhancement between mismatched and perfectly matched targets. A diminished relative fluorescence enhancement rate indicates enhanced specificity, as it suggests a greater capacity to distinguish between mismatched and matched targets. Our findings reveal that the detection sensitivity for single-point mutations was position-dependent in both the SCas12aV2 assay and the DETECTR system when compared to the wild-type target. Notably, the S6 ssDNA activator outperformed the S6.1 dsDNA-ssDNA hybrid in SNP detection. Specifically, mutations at positions M4, M6-9, and M10 substantially reduced the SCas12aV2-mediated *trans*-cleavage activity.

The conventional Cas12a system relies on precise base pairing within the 5-10 bp PAM-proximal seed region for DNA cleavage, exhibiting minimal tolerance for mismatches. This limitation is significant because genomic databases reveal that fewer than 5% of gene point mutations occur near PAM sequences. In contrast, our research demonstrates that the SCas12aV2 system not only recognizes single SNPs within the PAM-proximal seed region but also exhibits specificity for point mutations in the PAM-distal region. This enhanced capability substantially broadens the applicability of the system. Moreover, the SCas12aV2 system enables the detection of challenging SNPs, including those involving wobble base pairs and those located in high GC sequence contexts. These advancements allow the SCas12aV2 system to accurately discriminate between various tumor mutation types in clinical settings. Collectively, these findings highlight the exceptional reliability of the SCas12aV2 assay in detecting SNPs within both RNA and DNA targets.

Application of the SCas12aV2 assay for practical studies

The accurate clinical identification of pathogen-induced infections necessitates the utilization of highly sensitive and rapid RNA detection methods. In this study, we validated the effectiveness of the SCas12aV2 assay in detecting viable bacterial populations ranging from 0% to 100%, as well as in

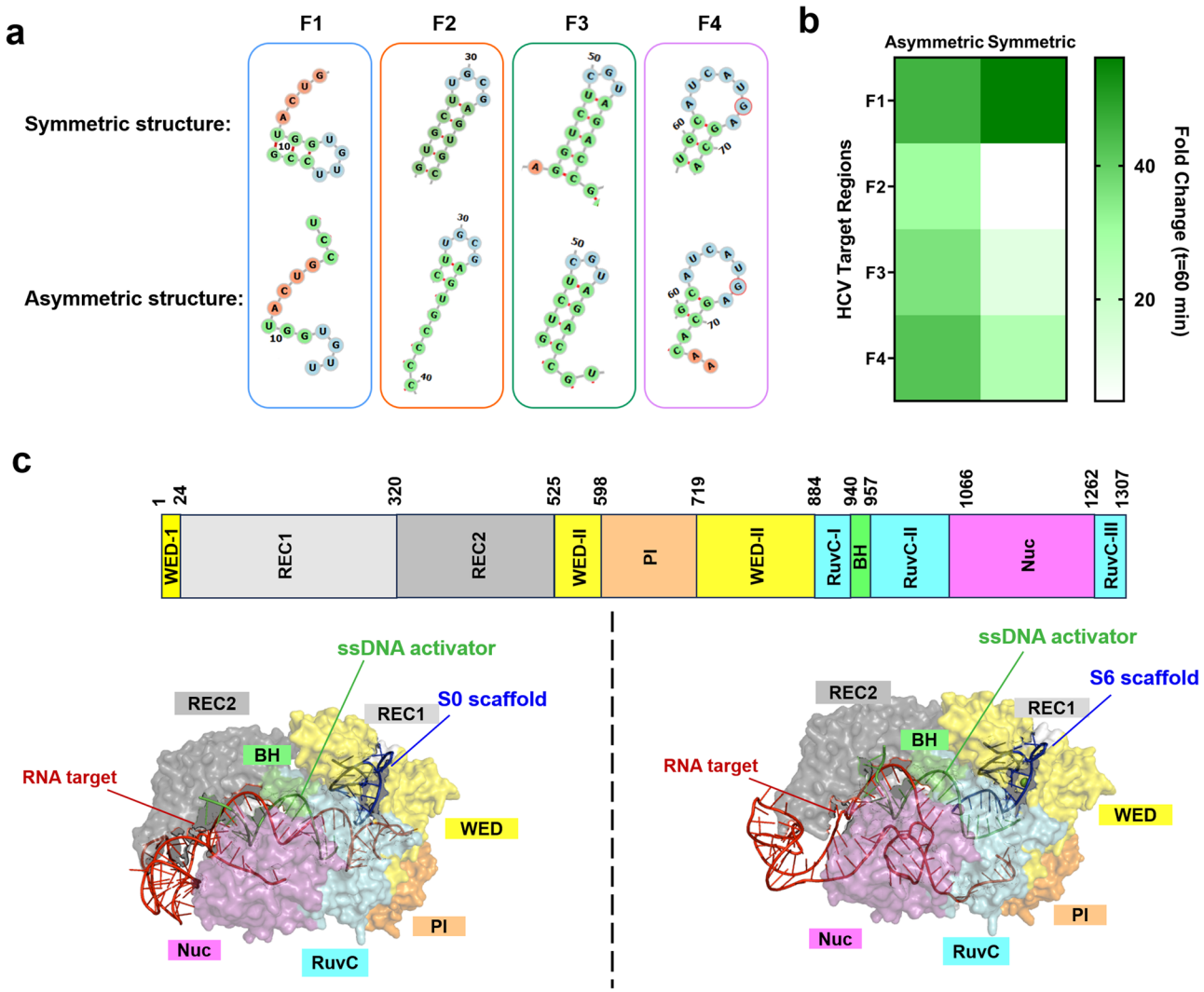


Fig. 4 | Detection of the symmetric or asymmetric structures of an HCV fragment by Cas12a complexed with S6 scaffold and ssDNA activator. a Schematic of an HCV RNA fragment with four target regions arranged symmetrically or asymmetrically. The predicted secondary structures were determined by NUPACK software. **b** Heat map representing fold change with respect to NTC at $t = 60$ min of an in vitro *trans*-cleavage fluorescence assay targeting the symmetric or asymmetric structures. **c** Overall structures of the AsCas12a/S0 scaffold+ssDNA/RNA target complex and AsCas12a/S6 scaffold+ssDNA/RNA target complex. Domains are colored according to the AsCas12a (PDB: 6GQZ). Supplementary Data 1 are provided as a Supplementary Data 1 file.

clinical specimens from individuals infected with SARS-CoV-2. Figure 9a depicts the preparation of bacterial suspensions containing varying proportions of viable and dead ATCC25922 *E. coli* within a volume of 1 mL. The *E. coli* viability assay can differentiate between viable and dead bacteria by assessing cell membrane integrity. Viable bacteria retain intact membranes, while dead bacteria exhibit membrane rupture, leading to the leakage and degradation of nucleic acids. Therefore, RNA detected in these assays serves as a marker exclusively for live bacteria, as dead bacteria are incapable of being cultured. Specifically, the ratio between viable and total bacteria was systematically adjusted from 0% to 100%. Initially, traditional plate counting techniques were employed to assess the viability of these samples by correlating colony counts with viable bacterial cell content (Fig. 9b). Subsequently, RNA extracted from these samples underwent SCas12aV2 analysis. A direct correlation was observed between fluorescence intensity and the proportion of viable bacteria (Fig. 9c). These findings demonstrate that the SCas12aV2 assay is capable of quantifying viable bacterial counts, exhibiting an enhanced ability to detect viable bacteria as the ratio between viable and total bacteria increases. Finally, we successfully isolated five RNA samples from nasal swab specimens collected from individuals confirmed to have SARS-CoV-2. The clinical RT-qPCR analysis yielded Ct values ranging from 10.87 to 22.23 for these samples. Employing the SCas12aV2 direct detection assay, which targets four distinct regions of the SARS-CoV-2 genome, we accurately identified all five samples as positive, with a clear distinction in slopes compared to the negative control swab depicted in Fig. 9e. The slopes of the positive samples were significantly correlated with their respective input concentrations, underscoring the assay's quantitative capability. The inclusion of a negative swab control enabled us to mitigate the impact of matrix effects inherent in clinical specimens. Additionally, we conducted tests with a non-targeting control S6.1 activator on all samples, which yielded no significant signals.

Discussion

This study introduces an innovative enhancement to the CRISPR/Cas12a-based detection system, specifically the SCas12aV2 assay, which holds significant potential for the precise detection of highly structured RNA molecules. To ensure the assay achieves high sensitivity and specificity, we systematically optimized the SCas12aV2 assay process in the following manner[1]: We initially evaluated the impact of different lengths of the ssDNA activator and found that the 20-nt activator achieved the optimal balance between activation efficiency and background signal[2]; Secondly, we

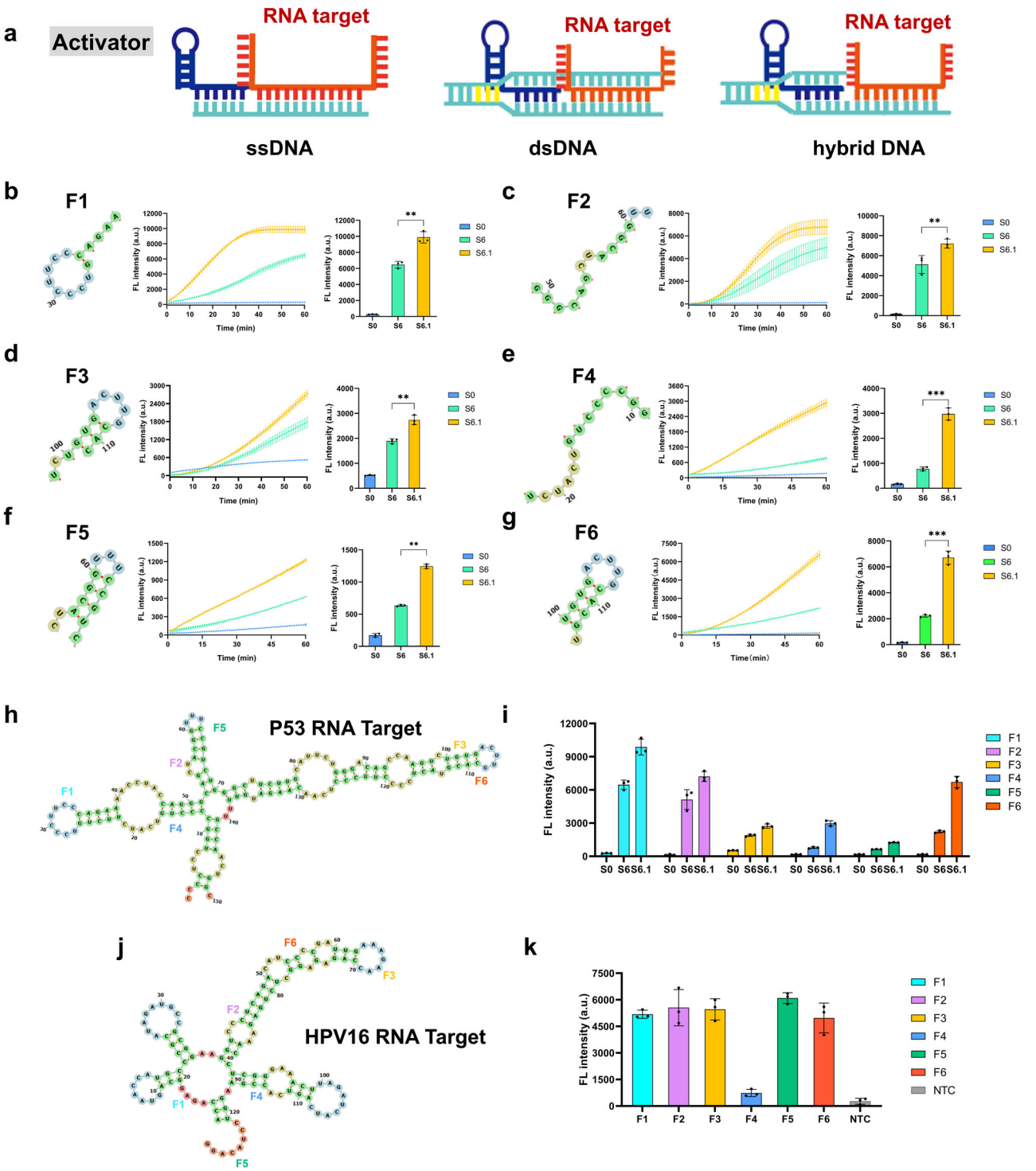


Fig. 5 | Detection of long RNA with complex structures utilizing dsDNA-ssDNA hybrid activators. a Schematic illustration of the SCas12a assay employing ssDNA, dsDNA, or dsDNA-ssDNA hybrid activators for RNA detection. **b–g** Comparison of the S0 (ssDNA), S6 (ssDNA) and S6.1 (dsDNA-ssDNA hybrid) DNA activators for in vitro *trans*-cleavage fluorescence assay. **h** The secondary structure of the TP53 RNA target was predicted using NUPACK software. **i** Comparative analysis of S0, S6, and S6.1 DNA activators targeting distinct regions of the TP53 RNA target. **j** The secondary structure of the TP53 RNA target was predicted using NUPACK software. **k** Comparative analysis of S0, S6, and S6.1 DNA activators targeting distinct regions of the HPV16 RNA target. For (**b**–**g**, **i**, and **k**), the reaction mixtures were incubated for 60 min at 37 °C and contained 250 nM of Cas12a enzymes, 500 nM S6 scaffold RNAs, 500 nM of DNA activators, 10 nM TP53 RNA targeted fragments and 1000 nM of fluorescent probes. All the experiments were conducted in triplicate and error bars represent mean value ± SD ($n = 3$). Supplementary Data 1 are provided as a Supplementary Data 1 file.

employed the software to predict the secondary structures and local free energy distribution of the target RNA. The results indicated that regions with higher free energy are less thermodynamically stable, making these areas more prone to disruption by activators and thus more suitable as target sites[3]; Finally, we conducted a series of experiments to determine the optimal buffer conditions that ensure both compatibility and high efficiency. These optimization strategies significantly improved the performance of the SCas12aV2 system. The key advantages of the SCas12aV2 assay can be summarized as follows[1]: it enables direct detection of highly structured RNA molecules without amplification, simplifying the process and reducing the

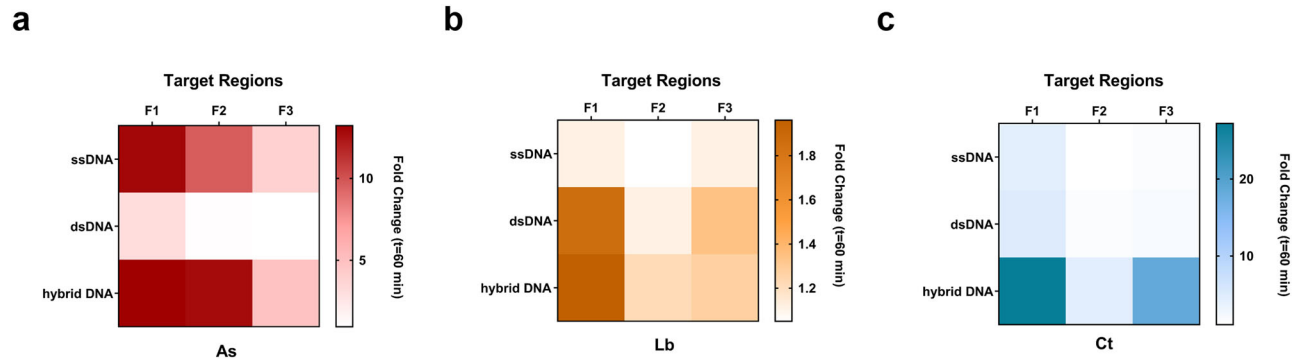


Fig. 6 | Validating the universality of SCas12aV2 assay by utilizing Cas12a orthologs. a–c Heat maps representing the fold changes in the fluorescence intensity of in vitro trans-cleavage assay ($n = 3$) with Cas12a orthologs. The reactions contained 250 nM of As, Lb, or Ct Cas12a enzymes, 500 nM S6 scaffold RNAs, 500 nM of ssDNA, dsDNA, or dsDNA-ssDNA hybrid activators, 10 nM TP53 RNA targeted fragments and 1000 nM of fluorescent probes. All the experiments were conducted in triplicate and error bars represent mean value ± SD ($n = 3$). Compared to the AsCas12a and LbCas12a assays, which were conducted at 37 °C, the CtCas12a assays were performed at a higher temperature of 55 °C. Supplementary Data 1 are provided as a Supplementary Data 1 file.

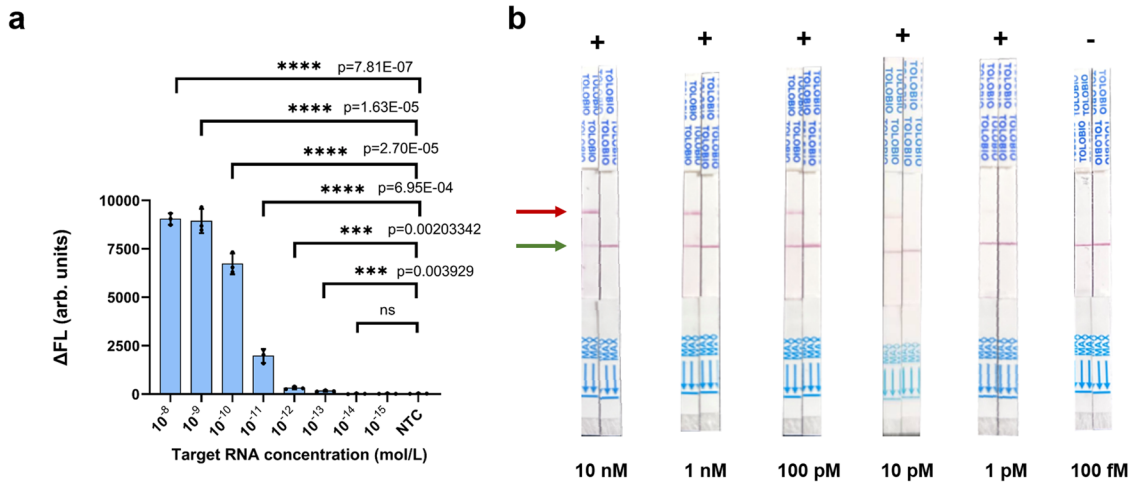


Fig. 7 | Determination of the limit of detection of the SCas12aV2 assay for RNA detection. a Limit of detection of the HIV target was determined by a fluorescence assay. The plot illustrates the background-subtracted fluorescence intensity at $t = 60$ min for varying concentrations of the target. All the experiments were conducted in triplicate and error bars represent mean value ± SD ($n = 3$), and statistical analysis was conducted using a two-tailed t-test. Statistical significance was determined as follows: ns (not significant) for $p > 0.05$, * for $p \leq 0.05$, ** for $p \leq 0.01$, *** for $p \leq 0.001$, and **** for $p \leq 0.0001$. **b** Limit of detection of the HIV target was determined by a lateral flow assay. Similar experiments were conducted, with the exception that a dipstick reporter was employed following a 60-min LFA cleavage reaction. The red arrow indicates the test bands, while the green arrow indicates the control bands. The results are denoted by the symbols "+" for positive outcomes and "-" for negative outcomes. Supplementary Data 1 are provided as a Supplementary Data 1 file.

risk of contamination and false positives[2]; it minimizes steric hindrance through structure-based design, including optimization of scaffold RNA length, targeting asymmetric RNA structures, and adopting a dsDNA-ssDNA hybrid as the activator to initiate *trans*-cleavage activity[3]; it is applicable to various Cas12 orthologs, including the thermostable CtCas12a, highlighting the assay's versatility and suitability for diverse conditions. Moreover, this method exhibits high sensitivity, achieving a LoD as low as 246 aM when using pooled DNA activators. Its specificity for SNPs confirms the assay's reliability in detecting SNPs within RNA targets. Additionally, the SCas12aV2 method accurately detects viable bacterial populations and RNA from clinical specimens, as evidenced by its application to SARS-CoV-2.

The SCas12aV2 assay, despite its significant enhancements, faces specific challenges. A primary limitation is the requirement for custom activator design for each target RNA, a process that can be time-consuming and may necessitate extensive optimization. Additionally, although the assay exhibits high sensitivity, it may struggle to distinguish between closely related sequences, potentially compromising its effectiveness in diagnostic applications where precise sequence recognition is critical. To address these issues, future iterations of the SCas12aV2 assay could integrate machine learning techniques to predict and optimize activator configurations, thereby streamlining the development process and reducing assay preparation times.

In conclusion, the SCas12aV2 assay constitutes a substantial advancement in molecular diagnostics, providing a sensitive, specific, and user-friendly method for the detection of structured RNA molecules. Its broad potential applications in research, clinical diagnostics, and infectious disease monitoring are evident. The "split-activator" system design has been validated for use with not only Cas12a orthologs but also other CRISPR/Cas enzymes, such as Cas13 and Cas14. We foresee the development of increasingly potent Cas enzyme-based detection tools in the future, advancing from the discoveries reported in this manuscript.

Methods

Ethical statement

For this study, human nasal swab specimens for SARS-CoV-2 detection were collected and provided by College of Medicine and Health Science with a protocol approved by the ethics committee at Wuhan Polytechnic University.

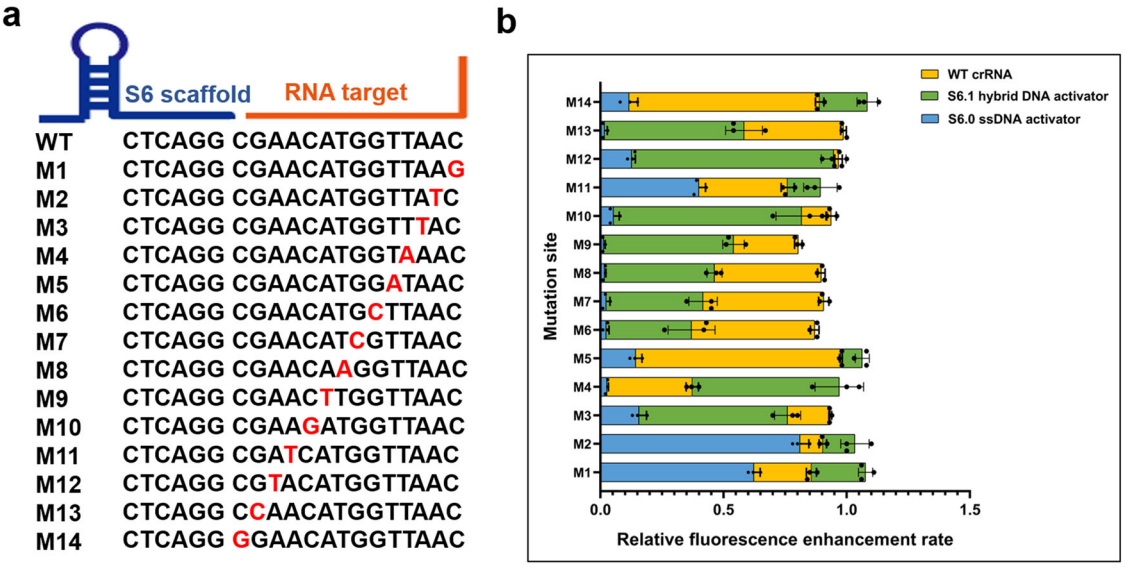


Fig. 8 | Specificity of SCas12aV2 assay towards single point mutations in target. a ssDNA activators were designed with point mutations across the length of the pairing region in an HIV target. The mutation location is identified by 'M' following the nucleotide number where the base has been changed to its complementary nucleotide (3' to 5' direction). **b** Comparison of fluorescence fold changes in the *trans*-cleavage assay between DETECTR and SCas12aV2 utilizing either S6 ssDNA or S6.1 hybrid DNA activators. All fluorescence values were normalized to those of WT activator. Statistical analysis for $n = 3$ biologically independent replicates comparing the normalized fold change for DETECTR vs SCas12aV2 assay. Statistical analysis was conducted using a two-tailed t test. Statistical significance was determined as follows: ns (not significant) for $p > 0.05$, * for $p \leq 0.05$, ** for $p \leq 0.01$, *** for $p \leq 0.001$, and **** for $p \leq 0.0001$. error bars represent mean value ± SD ($n = 3$). Supplementary Data 1 are provided as a Supplementary Data 1 file.

Materials

Fluorescence-based detection reagents, including DNA, RNA, FAM-tagged ssDNA, and FAM-tagged RNA, were sourced from Sangong Biotech (Shanghai, China) as detailed in Supplementary Table S1–S3. Buffer reagents were procured from Sinopharm (Beijing, China). Enzymatic reactions were facilitated by the use of 10 x NEB buffer 2.1 and 10 x Cutsmart buffer, both of which were supplied by New England Biolabs (Beijing, China). The cell transfection reagent Mergene 1000@HeLa was purchased from Pricella (Wuhan, China). The enzymatic degradation of proteins was carried out using proteinase K, and total RNA was isolated using a kit, both products being from Takara (Dalian, China). The experiments were conducted using ultrapure water to ensure the integrity of the reactions. Prior to use, all DNA and RNA molecules were resuspended in DEPC-treated water to eliminate RNase activity and then preserved at −20 °C for future experimental procedures.

Recombinant Cas12a orthologs and LwaCas13a protein expression and purification

Synthetic genes encoding the CRISPR-associated proteins AsCas12a, LbCas12a, CtCas12a, and LwaCas13a were cloned into the pET-28a(+) expression vector to construct plasmids for recombinant protein production. The sequence accuracy of these plasmids was verified prior to transformation into *Escherichia coli* BL21 (DE3) competent cells. For expression, a single colony was inoculated into LB broth supplemented with ampicillin (100 μg/mL) and incubated overnight. The following day, these cultures were diluted into 1-liter Terrific Broth (TB) medium to an optical density at 600 nm (OD_{600}) of 0.8, cooled on ice for 10 min, induced with 0.5 mM isopropyl β-D-1-thiogalactopyranoside (IPTG), and further incubated at 18 °C for 16 h. The bacterial cells were then pelleted by centrifugation and lysed in buffer A (20 mM Tris-HCl, pH 7.5, 300 mM NaCl, 1 mM phenylmethanesulfonyl fluoride (PMSF), 5 mM β-mercaptoethanol) containing a cocktail of proteinase inhibitors. The recombinant Cas proteins were purified using immobilized metal affinity chromatography (IMAC) with Ni-NTA resin, followed by size-exclusion chromatography on a HiLoad® 16/600 Superdex® column as per a published protocol[22]. The purified proteins were concentrated using a 100 kDa molecular weight cut-off (MWCO) centrifugal filter and their concentrations determined by the Bradford assay. Subsequently, the concentrated proteins were flash-frozen in liquid nitrogen and stored at −80 °C for subsequent applications.

Gel electrophoresis

Reconstitution of wild-type Cas12a and SCas12aV2 ribonucleoproteins was achieved by mixing the respective Cas12a nucleases with either full-length crRNA or split crRNA at a 1:2 molar ratio in a reaction buffer, followed by a 20-min incubation at ambient temperature. To assess the *trans*-cleavage activity of both wild-type Cas12a and SCas12aV2 RNPs, experiments were conducted under identical conditions as previously detailed[22], with the exception of the inclusion of a 20 nM concentration of a 42-nt ssDNA reporter. This reporter was mixed with either 10 nM of 59-bp dsDNA targets (Fig. 2a) or 59-nt ssDNA targets (Fig. 2b). The reaction outcomes were resolved on a 12% polyacrylamide gel, utilizing 1X TBE buffer for electrophoresis at a steady voltage of 100 V over a period of 2 h. Subsequently, the gel was visualized by staining with GoldView nucleic acid stain and examined under UV illumination for documentation.

Application of the SCas12aV2 fluorescence assay for RNA detection

Fluorescence-based detection assays were performed using a CFX96 touch real-time PCR system (Bio-Rad, Hercules, CA, USA). The assays began with the preparation of a reaction mixture consisting of 250 nM Cas12a, 500 nM scaffold RNA, and 500 nM of either ssDNA, dsDNA, or dsDNA-ssDNA hybrid activators. The components were mixed in NEB buffer 2.1 and nuclease-free water, followed by a 10-min incubation at room temperature to allow equilibration. Next, 1000 nM FQ reporter and the appropriate concentration of target RNA were added to each reaction, bringing the total volume to 20 μl. The reactions were then incubated at 37 °C for 60 min, monitoring the fluorescence emission at 520 nm. For LwaCas13a-mediated assays, the protocol was identical, except for the use of a FAM-ssRNA reporter.

In parallel, lateral flow assays were conducted with a dipstick containing ssDNA probes for detection. The LFA dipsticks, obtained from ToloBio (Shanghai, China), incorporated a FAM-biotin reporter for

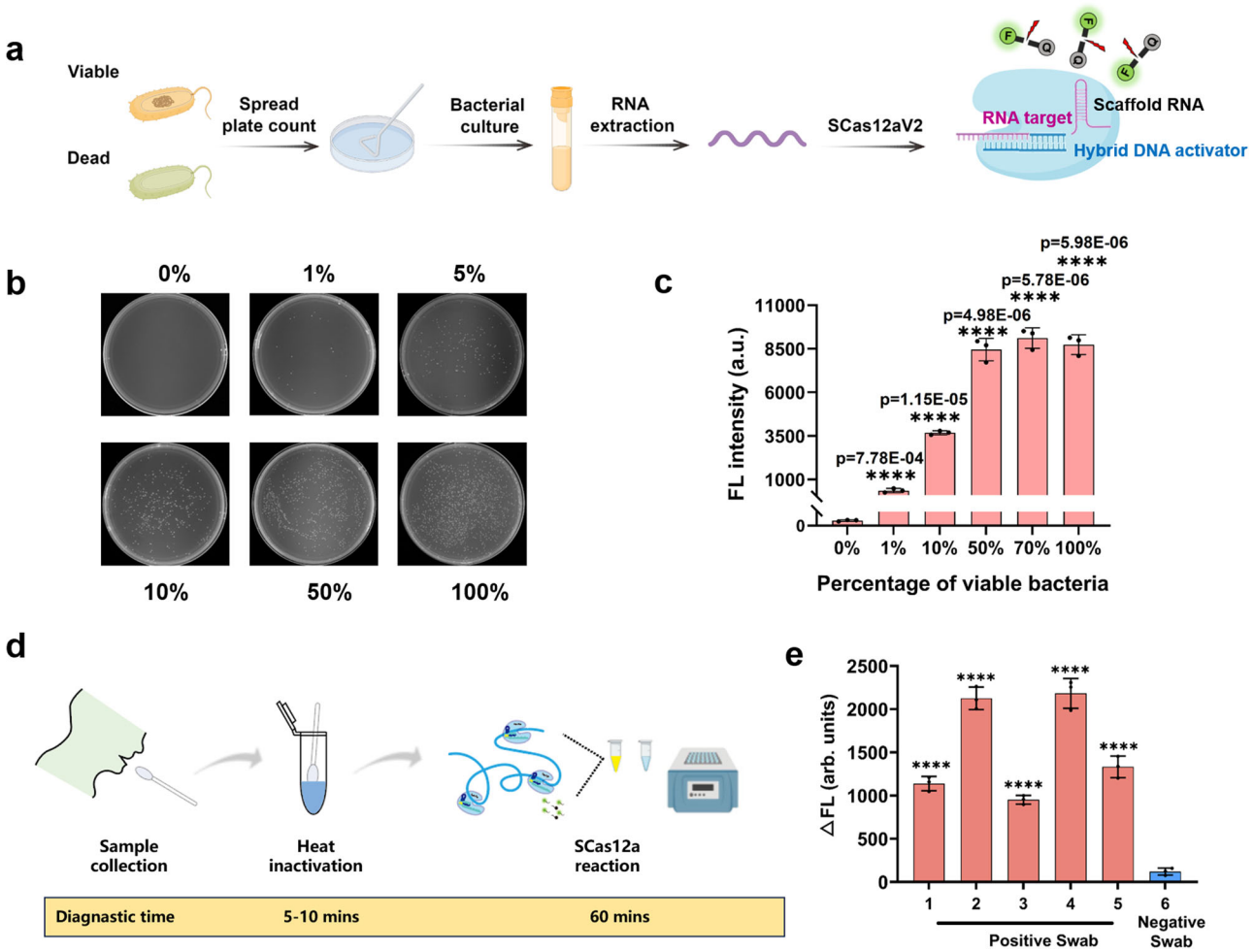


Fig. 9 | Utilization of the SCas12aV2 assay for pathogen detection. a Schematic diagram of differentiating ATCC25922 *E. coli* viable and dead bacteria by SCas12aV2 assay. **b** The ratio of viable bacteria to total bacteria was verified using standard plate counts as 0, 1, 5, 10, 50, and 100%, respectively. **c** Analyzing viable pathogenic bacteria using the SCas12aV2 assay. The fluorescence response of SCas12aV2 was assessed for profiling bacteria at various percentages of viable bacteria (0, 1, 5, 10, 50, and 100%). The reaction employed *E. coli* 16S rRNA primer1, 1 μM *E. coli* 16S rRNA primer2, and *E. coli* 16S rRNA targeted S6.1 activator, respectively. **d** Schematic diagram of detecting SARS-Cov-2 from the clinical swab samples by SCas12aV2 assay. **e** Pre-extracted RNA from five nasopharyngeal swabs confirmed positive for SARS-CoV-2 by RT-qPCR was tested by SCas12aV2 assay. A confirmed negative swab was tested for comparison. All fluorescence values were normalized to those of WT activator. Statistical analysis for $n = 3$ biologically independent replicates comparing the normalized fold change for DETECTR vs SCas12aV2 assay. Statistical analysis was conducted using a two-tailed t-test. Statistical significance was determined as follows: ns (not significant) for $p > 0.05$, * for $p \leq 0.05$, ** for $p \leq 0.01$, *** for $p \leq 0.001$, and **** for $p \leq 0.0001$. error bars represent mean value ± SD ($n = 3$). Supplementary Data 1 are provided as a Supplementary Data 1 file.

immunochromatographic analysis. In negative samples, the gold particle-biotin antibody complex bound to the FAM-biotin reporter, which was captured by the anti-FAM antibody on the test strip. Positive samples, however, exhibited cleavage of the FAM-biotin reporter by active Cas12a, resulting in a visible concentration of the gold particle-biotin antibody complex on the test line and a diminished signal on the control line.

RNA extraction and RT-qPCR for detection of RNA

RNA was extracted from ATCC25922 *E. coli* and SARS-CoV-2 lysis via the RNA extraction kit from GenePharma (Suzhou, China). Next, the cDNA was synthesized from the extracted total RNA using the miRCURY LNA RT Kit (Qiagen). Briefly, a reverse transcription reaction was performed at 42 °C for 60 min and then inactivated at 95 °C for 5 min. Synthesized cDNA was stored at −20 °C before use. For the detection of specific RNA targets, the primers and RT-qPCR detection kit were designed and ordered from GenePharma (Suzhou, China). Subsequently, the RNA targets in the biological samples were quantitatively assessed according to the protocol provided by the manufacturer. The real-time quantitative polymerase chain reaction (RT-qPCR) reactions were performed using a CFX96 touch real-time PCR system (Bio-Rad, CA, USA) and the RNA targets were identified utilizing the SYBR green fluorescent method. The thermal cycling conditions included an initial denaturation step at 94 °C for 3 min, followed by 40 cycles of denaturation at 94 °C for 12 s and annealing/extension at 62 °C for 30 s.

Limit of detection calculation

The limit of detection (LoD) was determined by conducting the trans-cleavage assay using various dilutions of RNA or DNA targets. The value of LOD was calculated by using formula 3σ/slope, where σ is the standard deviation of three blank solutions.

Statistics and reproducibility

No statistical method was used to predetermine sample size. A minimum of three independent replicate experiments were conducted. No data were excluded from the analyses. The experiments were not randomized. The Investigators were not blinded to allocation during experiments and outcome assessment.

Reporting summary

Further information on research design is available in the Nature Portfolio Reporting Summary linked to this article.

Data availability

All the data supporting the findings of this study are available within the Article and Supplementary Files. Source data are provided in Supplementary Data 1

Received: 25 October 2024; Accepted: 25 February 2025;
Published online: 04 March 2025

References

1. Kaminski, M. M., Abudayyeh, O. O., Gootenberg, J. S., Zhang, F. & Collins, J. J. CRISPR-based diagnostics. *Nat. Biomed. Eng.* **5**, 643–656 (2021).
2. Weng, Z. et al. CRISPR-Cas biochemistry and CRISPR-based molecular diagnostics. *Angew. Chem. Int. Ed. Engl.* **62**, e202214987 (2023).
3. Chen, J. S. et al. CRISPR-Cas12a target binding unleashes indiscriminate single-stranded DNase activity. *Science* **360**, 436–439 (2018).
4. Li, S. Y. et al. CRISPR-Cas12a-assisted nucleic acid detection. *Cell. Disco.* **4**, 20 (2018).
5. Zetsche, B. et al. Cpf1 is a single RNA-guided endonuclease of a class 2 CRISPR-Cas system. *Cell* **163**, 759–771 (2015).
6. Broughton, J. P. et al. CRISPR-Cas12-based detection of SARS-CoV-2. *Nat. Biotechnol.* **38**, 870–874 (2020).
7. Feng, W. et al. Integrating reverse transcription recombinase polymerase amplification with CRISPR technology for the one-tube assay of RNA. *Anal. Chem.* **93**, 12808–12816 (2021).
8. Zhang, W. S. et al. Reverse transcription recombinase polymerase amplification coupled with CRISPR-Cas12a for facile and highly sensitive colorimetric SARS-CoV-2 detection. *Anal. Chem.* **93**, 4126–4133 (2021).
9. Yan, H. et al. A one-pot isothermal Cas12-based assay for the sensitive detection of microRNAs. *Nat. Biomed. Eng.* **7**, 1583–1601 (2023).
10. Rananaware, S. R. et al. Programmable RNA detection with CRISPR-Cas12a. *Nat. Commun.* **14**, 5409 (2023).
11. He, W. et al. Split activator of CRISPR/Cas12a for direct and sensitive detection of microRNA. *Anal. Chim. Acta.* **1303**, 342477 (2024).
12. Moon, J. & Liu, C. Asymmetric CRISPR enabling cascade signal amplification for nucleic acid detection by competitive crRNA. *Nat. Commun.* **14**, 7504 (2023).
13. Chen, Y. C. et al. Split crRNA with CRISPR-Cas12a enabling highly sensitive and multiplexed detection of RNA and DNA. *Nat. Commun.* **15**, 8342 (2024).
14. Gootenberg, J. S. et al. Multiplexed and portable nucleic acid detection platform with Cas13, Cas12a, and Csm6. *Science* **360**, 439–444 (2018).
15. Kellner, M. J., Koob, J. G., Gootenberg, J. S., Abudayyeh, O. O. & Zhang, F. SHERLOCK: nucleic acid detection with CRISPR nucleases. *Nat. Protoc.* **14**, 2986–3012 (2019).
16. Wang, T. et al. SATCAS: A CRISPR/Cas13a-based simultaneous amplification and testing platform for one-pot RNA detection and SNPs distinguish in clinical diagnosis. *Biosens. Bioelectron.* **263**, 116636 (2024).
17. Fozouni, P. et al. Amplification-free detection of SARS-CoV-2 with CRISPR-Cas13a and mobile phone microscopy. *Cell* **184**, 323 (2021).
18. Huang, S., Lou, T. L. & Zheng, L. Synergistic effect of split DNA activators of Cas12a with exon-unwinding and induced targeting effect. *Nucleic. Acids. Res*. **52**, 11148–11157 (2024).
19. Kleinstiver, B. P. etal. Genome-wide specificities of CRISPR-Cas Cpf1 nucleases in human cells. *Nat. Biotechnol.* **34**, 869 (2016).
20. Wu, J. et al. Characterization of a thermostable Cas12a ortholog. *Cell. Insight.* **2**, 100126 (2023).
21. Zhang, J. Y. et al. Intrinsic RNA Targeting Triggers Indiscriminate DNase Activity of CRISPR-Cas12a. *Angew. Chem. Int. Ed.* **63**, e202403123 (2024).
22. Qiao, J. et al. Co-expression of Cas9 and single-guided RNAs in *Escherichia coli* streamlines production of Cas9 ribonucleoproteins. *Commun. Biol.* **2**, 161 (2019).

Acknowledgements

This work was supported by the National Key Research and Development Program of China 2022YFC2304304 (Y.L.), Science and Technology Innovation Talent Plan of Hubei Province 2023DJC136 (Y.L.), the Open Funding Project of the State Key Laboratory of Esophageal Cancer Prevention K2022-008 (J.Q.), the Open Funding Project of the State Key Laboratory of Biocatalysis and Enzyme Engineering SKLBEE2022022 (J.Q.), Research Funding of Wuhan Polytechnic University NO.2022RZ031 (J.Q.).

Author contributions

J. Qiao, J. Q. Zhang, W.X. Mao, and Y. Liu designed research; J. Q. Zhang, W. H. Yin, Q. Y. Jiang, S.Q. Jin, P.X. Wang and W. W. Deng performed research; P.X. Wang and R. Y. He collected the patient samples; J. Q. Zhang, Q. Y. Jiang and Y. Liu analyzed data; and Y. Liu wrote the paper.

Competing interests

Yi Liu is a professor of bioscience at Hubei university, and a scientific advisor to BravoVax. The regents of Hubei University and BravoVax have one patent pending for CRISPR-Cas12a detection technologies on which professor Yi Liu and Jie Qiao are inventors. The remaining authors declare no competing interests.

Additional information

Supplementary information The online version contains supplementary material available at https://doi.org/10.1038/s42003-025-07806-5.

Correspondence and requests for materials should be addressed to Wuxiang Mao, Jie Qiao or Yi Liu.

Peer review information *Communications Biology* thanks Guoliang Ke and the other, anonymous, reviewers for their contribution to the peer review of this work. Primary Handling Editors: Mengtan Xing and Rosie Bunton-Stasyshyn. A peer review file is available.

Reprints and permissions information is available at http://www.nature.com/reprints

Publisher's note Springer Nature remains neutral with regard to jurisdictional claims in published maps and institutional affiliations.

Open Access This article is licensed under a Creative Commons Attribution-NonCommercial-NoDerivatives 4.0 International License, which permits any non-commercial use, sharing, distribution and reproduction in any medium or format, as long as you give appropriate credit to the original author(s) and the source, provide a link to the Creative Commons licence, and indicate if you modified the licensed material. You do not have permission under this licence to share adapted material derived from this article or parts of it. The images or other third party material in this article are included in the article's Creative Commons licence, unless indicated otherwise in a credit line to the material. If material is not included in the article's Creative Commons licence and your intended use is not permitted by statutory regulation or exceeds the permitted use, you will need to obtain permission directly from the copyright holder. To view a copy of this licence, visit http://creativecommons.org/licenses/by-nc-nd/4.0/.

© The Author(s) 2025